ORIGINAL PAPER

The influence of shear on the dewatering of high consistency nanofibrillated cellulose furnishes

**Katarina Dimic-Misic · Antti Puisto ·
Jouni Paltakari · Mikko Alava ·
Thaddeus Maloney**

Abstract This paper demonstrates a way to utilize the rheological properties of high consistency microfibrillated and nanofibrillated cellulose (MFC and NFC) based furnishes for improved dewatering. This is relevant to a new manufacturing platform that is being developed to form composite webs from suitable mixtures of MFC or NFC, traditional pulp fibres and pigments. The studied furnishes were evaluated in the consistencies range of 5–15 % with an MCR 300 rheometer and an immobilization cell. This setup enables us to characterize the rheology of the samples before and during the dewatering process. Classical rheological methods are used to characterise MFC and NFC furnishes. Yield stress as an indicator of the flocculated network strength was found to increase with the consistencies, following the increase in elastic moduli, which indicated a gel-like strongly flocculated matrix. The shear thinning properties of furnishes are observed to follow the Oswald's rheological model on a wide range of shear rates. It was found that when the MFC and NFC furnishes were dewatered under vacuum conditions, the final solids content was increased with application of shear. This behaviour is more pronounced for furnishes which contained the more swollen NFC (higher WRV, i.e. higher zeta potential). This effect is further exemplified by the change of the complex and dynamic viscosities during the dewatering. The shear rate, the fibre content, and the furnish consistencies were also found to influence the dewatering rate.

Keywords Nanofibrillated cellulose ·
Microfibrillated cellulose · Rheology · Shear-
thinnning · Dewatering · Immobilization cell

Introduction

The objective of this research is to develop an understanding of the rheological and dewatering properties of nanocellulose composite furnishes in the high consistencies range. Furnishes containing a high fraction of pigment for light scattering, a moderate amount of nanocellulose for bonding, and a smaller amount of traditional pulp fibres for reinforcement have been the subject of interest in recent years (Subramanian et al. 2011). Various types of composite materials can be produced from such furnishes if an efficient manufacturing strategy can be developed. Since a furnish which may contain 10–20 % nanocellulose has an inherently poor dewatering, it is our belief that webs which will be produced at relatively high consistency

K. Dimic-Misic (✉) · J. Paltakari · T. Maloney
Department of Forest Products Technology,
School of Chemical Technology, Aalto University,
PO Box 16300, 00076 Aalto, Finland
e-mail: katarina.dimic.misic@aalto.fi

A. Puisto · M. Alava
Department of Applied Physics, School of Science,
Aalto University, PO Box 14100, 00076 Aalto, Finland

would utilize novel dewatering strategies, other than those used at traditional paper machines. For this reason we believe that it is important to develop a deeper understanding of the rheology and dewatering characteristics of high consistency nanocellulose-based furnishes.

In this article "nanocellulose" refers generically to the material resulting when traditional chemical pulp fibres are defibrillated either by chemical or mechanical means (Siró and Plackett 2010). Depending on the defibrillation route, pulp fibres may be broken down to elementary fibrils in the size approaching 4 nm or fibril aggregates ranging approximately 10–50 nm in width. Major diversity is found in raw materials used for the productions of nanofibrillated cellulose and they all possess many special properties compared to traditional pulp fibres; a much higher surface area, great bonding potential, and a high water binding capacity (Agoda-Tandjawa et al. 2012; Turbak et al. 1984).

Microfibrillated cellulose (MFC) can be prepared from chemical pulps by mechanical shearing (Henriksson et al. 2007). Depending on the amount of energy used and the way in which it is applied, various size distributions of fibril aggregates can be produced. If the pulp fibres are oxidized to increase the charge on the cellulose, the fibres can be more easily broken down to a finer distribution of fibrils approaching the elementary fibril width of about 4 nm. The TEMPO mediated (Lasseuguette et al. 2008) process for the production of nanofibrillated cellulose (NFC) is currently the focus of research. MFC and NFC represent fairly distinct categories of nanocellulose, each having potential commercial applications. In water dispersions, at concentrations of approximately 1 % solids and higher, nanocellulose forms a highly entangled network consisting of nanoscale size elements with a gel-like behaviour (Nakagaito et al. 2009); (Iotti et al. 2011). The typical size of NFC is smaller and surface charge much higher compared to MFC. As a result, NFC forms a gel at much lower concentrations. In other words, it binds more water and has higher swelling than MFC. Effect of swelling of fibers on their rheological behaviour has been widely studied (Horvath and Lindström 2007); (Lindström and Carlsson 1982), and it is apparent that the difference in swelling between MFC and NFC should strongly influence the rheology and dewatering behaviour of furnish.

Different approaches to dewatering of papermaking furnishes have been the subject of intense research for many decades. Both experimental techniques and mathematical models have been developed to describe the water removal in all stages of the paper machine, from the initial forming section through vacuum boxes into press and final thermal water removal (Hubbe and Panczyk 2007; Paradis et al. 2002). Although the composition of papermaking furnishes vary greatly, the main components are the relatively mobile, limitedly swollen fibres, a small amount of more mobile swollen fines, and a variable amount of inorganic non-swelling pigment. The dewatering strategy implemented on a given paper machine is highly dependent on its ability to transport water through the fibre network out of the web at all phases of water removal (Hubbe and Panczyk 2007). Some research suggests, that "sheet sealing", where small particles tend to plug the wire during vacuum dewatering, can be avoided by the judicious application of positive vacuum pulses (Hubbe and Heitmann 2007). However, other studies do not find such an effect with traditional furnishes (Pujara et al. 2008); (Raisanen et al. 1995). If the sheet permeability is lost during any phase of water removal, the efficiency will be greatly reduced and the energy consumption increased.

The types of furnishes we are observing in this study are high consistency furnishes that contain 70 % pigment, 20–30 % nano and/or microfibrillated cellulose and 0–10 % pulp fibres. This is clearly a challenging furnish to dewater, since it contains high amount of fibrillar cellulose material, clearly requiring a different dewatering strategy than those used for cellulose based high consistency papermaking furnish. In this case, water (in liquid or vapour form) must pass through relatively small channels around fibrils and pigments. When there is a static dewatering pressure, a low permeability is expected, anticipating difficult dewatering. However, if permeability is formed into the web by continuously disrupting the flow channels by the application of mechanical forces, it appears to be possible to improve the dewatering characteristics of furnish. It is this latter idea and hypothesis that we wish to explore in this study.

The use of rheology for the characterisation of MFC/NFC furnishes has been the subject of numerous studies in the last years (González et al. 2012). Although many studies relating rheological analyses to dewaterability have been conducted (Blanco et al.

2007), the rheological measurements and the dewatering (drainage) tests have often been conducted separately (Paradis et al. 2002). In this study, a novel methodology has been developed to study furnish rheology and dewatering simultaneously. An immobilization cell (IMC) is coupled with a dynamic mechanical rheometer for evaluation of the effect of shear as well as the increase in solid content during dewatering (Dursun and Dentel 2008; Willenbacher et al. 1999). Earlier this device has mainly been applied to the study of coating colour dewatering (Jäder et al. 2003; Willenbacher 2011; Wollny 2001) and recently to bio sludge dewatering (Ayol et al. 2010; Dursun and Dentel 2008). The measurement should also be applicable to all dewatering processes with viscoelastic fluids. Therefore, in this work, the IMC method is used to study the rheological and dewatering behaviour of nanocellulose based furnishes under applied shear and vacuum. Shear thinning behaviour of microfibrillar and nanofibrillar material is found to be the governing property influencing the shear-induced dewatering.

Experimental

Materials used

The filler was a commercial undispersed precipitated calcium carbonate with scalenohedral morphology (SPCC). The particle size was 4.3 μm measured with Malvern dynamic light scattering. A commercial bleached pine Kraft bale pulp was refined to a Shopper-Riegler number of 24 with a Valley Beater. MFC was produced from never-dried bleached Birch Kraft pulp. The defibrillation was carried out by passing the pulp three times through a Masuko grinder at 3 % solids (Karppinen et al. 2011). The Brookfield (vane) (Barnes and Carnali 1990)viscosity at 10 rpm of the MFC was 23,000 mPas at 1.5 % solids. The measured zeta potential was −24.3 mV at pH 9.5. The transmittance for 0.1 % consistency for the wavelength of 800 nm was 34 % (Chinga-Carrasco et al. 2012).

The applied NFC sample was a semi-commercial one, produced with the TEMPO process (Saito and Isogai 2005) from the never dried birch pulp. The Brookfield (vane) viscosity of the NFC at 1.5 % solids at 10 rpm was 46,657 mPas. The measured zeta potential was −57 mV at pH 9.2.

Furnishes were made for three consistencies 5, 10 and 15 % solids content. The furnish composition was 70 % filler, 20–30 % MFC or NFC, and 0–10 % cellulose fibres. All the labels follow the notation: ratio of pigment/ratio and type of nanocellulose/ratio of pulp/consistency. The MFC or NFC was mixed with filler at vigorous rotation with laboratory Diaf mixer for 25 min and the cellulose pulp was added to this suspension with further mixing at the same mixer as above. De-ionized water was used for dissolution and preparation throughout the study. The samples were stored in cold at 5 °C temperature.

The swelling of MFC and NFC was evaluated with a modified water retention test WRV ISO/DIS 23,714: Pulps measurement. Modification of this test was that we had mixed different contents of nanocellulose and kraft pulp in pads and measured WRV of such pads. Nanocellulose content in the pad was 0, 2, 4 and 6 %, respectively. Therefore we used WRV curves obtained from this measurements and the incremental contribution of nanocellulose to the WRV to evaluate its swelling. In such a way we obtained apparent WRV. We used WRV versus nanocellulose content in order to define maximum amount of nanocellulose in pad which gives good estimation of swelling for both MFC and NFC, and that was later referred to apparent WRV.

Rheological measurements

All rheological measurements were performed at the room temperature. For each measurement a new sample was used, and the mean values of ten successive measurements were used for calculation of the experimental data.

Physica MCR-300 rheometer was used in controlled shear mode with plate–plate geometry. The rheometer was equipped with 25 mm plate–plate geometries with both upper and lower surface profiled (serrated) with a 0.5 mm deep texture. The gap was initially set to 1 mm and the sample was allowed to rest for 10 min before starting the measurement. The temperature was set to a constant value of 23 °C. Both MFC suspensions and MFC furnishes were measured applying a strain sweep, frequency sweep, direct strain-controlled oscillatory (DSO) mode, and shear flow in CSR mode. In the strain sweep the strain was varied between 0.1 and 500 % and the angular frequency was set to 1 Hz. Next, the frequency sweep was conducted after determining the linear viscoelastic region, using the

amplitude sweep at 0.2 % strain with varying angular frequency from 100 to 0.01 Hz. Dynamic viscosity as a function of shear rate was measured at a steady state flow by increasing the shear rate from 0.01 to $1,000 \, s^{-1}$. Note that the present geometry is very prone for shear inhomogeneities such as shear banding due to the inherent shear gradient in the radial direction (Ovarlez et al. 2009). This is especially true for shear thinning complex fluids such as nanocellulose. Furthermore, is well documented in the literature, that vacuum filtration induces a gradient in the solid content in the filter normal direction (Jäder et al. 2003). Therefore, all the rheological properties of the samples measured in this way correspond to their apparent values specific for this geometry and are suitable only for comparative studies.

Yield stress

The yield stress was determined from the amplitude sweep data for the storage modulus G′ as explained in the literature (Agoda-Tandjawa et al. 2012; Horvath and Lindström 2007; Walls et al. 2003). As pointed out by many authors, the apparent yield stress depends on the method by which it is determined as well as the flow geometry (Barnes 2007; Renardy 2010). Therefore, the yield stress is not necessarily unique for a particular fluid. However, fixing the measuring protocol allows us to compare the two furnishes. From the amplitude sweeps curves one can obtain the *plateau value* $G_0′$. Above *critical strain* Υ_c, the storage modulus starts to decrease at the point of the breakage of the network structure.

Yield stress (τ_c) is calculated as the product of the storage modulus in the linear region and the critical strain, as presented in Eq. 1.

$$\tau_c = G_0′\gamma_c \tag{1}$$

Shear thinning-shear behaviour

The influence of shear rate on the variation of viscosity was observed by measuring the steady state flow curve using an MCR300 rheometer in the CSR mode at the shear rate range $0.1–1,000 \, s^{-1}$ (including data between 2 and $20 \, s^{-1}$) (Karppinen et al. 2011; Lasseuguette et al. 2008), (Iotti et al. 2011; Richmond 2012). Oswald de-Waele (Power Law) empirical model was fitted against the experimental data (Dolz

et al. 1994; Lasseuguette et al. 2008; Richmond 2012) at the range $1–1,000 \, s^{-1}$ allowing the comparison of the power-law coefficients between the furnishes at different concentrations.

IMC-immobilization cell dewatering

Dynamic dewatering measurement was conducted using a *Physica MCR 300 rheometer with IMC* accessory as licensed from BASF-AG. The cell consists of a stainless steel cylindrical metal tube with a punched metal plate that allows drainage of water through the samples (Willenbacher 2011; Wollny 2001). A filter is fastened on the top of the metal plate and the furnish to be investigated is applied. The upper plate is then lowered into contact with sample which is then pre-sheared. The sample is dewatered through the filter by vacuum suction. The normal forces of the sample tend to push upper rotating plate and, as dewatering occurs, the normal force tends to decrease. The axial force acting on the upper plate is set to a constant value, as described by other authors (Jäder and Järnström 2003) By setting axial force acting on the upper plate to constant (here to 0), the upper plate moves down thus decreasing the gap between the plates, i.e. compensating for the dewatered volume of the filtrate. At some point, the flow from the sample decreases, normal force becomes constant and viscosity becomes linear. A parallel plate geometry measuring system (PP-50) with a 50 mm diameter was used in all immobilization tests and initial gap was set to 1 mm (Wollny 2001). Different filter paper and membrane types were tested. The most reproducible results were obtained by using a Whatman nuclepore membrane, with the pore size of 0.2 μm. For the purpose of this study we modified a traditional IMC measurement used for coating colour dewatering (Jäder et al. 2003; Pajari and Koskela 2010; Wollny 2001) .

Two testing approaches can be applied with the IMC: the controlled shear rate (CSR) and the direct strain-controlled oscillatory (DSO) method. Dewatering with the DSO method provides viscoelastic properties of the sample (storage (G′), loss moduli (G″) and the loss factor (tan δ)) (Wollny 2001). The tan δ, which is the ratio of G″/G′, marks the transition of liquid like to solid-like behaviour during dewatering (Wollny 2001). However, during the CSR tests, the viscoelastic properties could not be determined,

instead only the change in dynamic viscosity could be monitored (Ayol et al. 2010).

In our dewatering models, DSO was used with the application of vacuum. CSR intervals were applied between the DSO intervals. Dewatering with vacuum was performed during the DSO intervals, due to the fact that applying vacuum during the CSR cycle would make the small particles to plug the filter pores. The samples were pre-sheared in the DSO cycle for 40 s, in the first interval, and then the periodic succession of DSO and CSR proceeded. During the DSO intervals vacuum dewatering was applied with the vacuum pressure of 50 mbar and the duration of 100 s. In-between the DSO intervals, the CSR intervals were applied while the vacuum pump was switched off manually, the duration of these intervals was 10 s. One measurement lasted 800 s consisting of with 14 intervals (pre-shearing DSO +7 DSO + 6 CSR).

Three different measurement schemes were performed, with different shear rates that were applied in the CSR intervals; shear rates being 0/40/200/ s^{-1}. The rotation rates were chosen based on exhaustive pre-tests: 40 s^{-1} was the minimum shear rate showing a clear increase in the solid content compared to the no-rotation, and 200 s^{-1} was the maximum shear rate that could be used for all the furnishes limited by the viscoelastic Weissenberg response, tending to increase the gap. The solids content of the pad after the dewatering was determined by gravimetric means. Final solid content for given furnish and dewatering model was calculated as the average of ten measurements from ten different pads.

Results and discussion

MFC/NFC specifications

The incremental change in the water retention value (WRV) of the furnish cake with different MFC/NFC content was used to calculate the fiber swelling. The values of the apparent WRV of 2 % MFC/NFC in furnish cake were used as the last values in the linear part of the apparent WRV curve, Fig. 1.

The WRV of MFC and NFC show nonlinear behaviour, which is most obvious in the case of NFC. This is due to a water transport issue—when the pad becomes too impermeable it can no longer be effectively dewatered in a centrifuge. Therefore, the
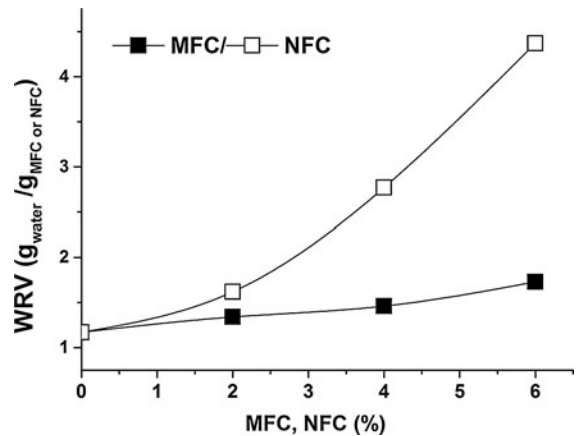

Fig. 1 The water retention value of furnish cakes with varying nanocellulose content. The NFC and MFC swelling, estimated at 2 % content, is 24 and 9 g water/g of nanocellulose, respectively

best estimate of the water holding capacity of the nanocellulose can be obtained at low nanocellulose contents; in this case we used 2 %. The apparent WRV calculated from Fig. 1 was 24 g water/g for NFC and 9 g/g for MFC. Due to its finer structure and higher charge the NFC has nearly three times the network level swelling of MFC. This should have a significant influence on furnish rheology and dewatering (Ramaswamy 2003; Spence et al. 2010).

The role of MFC/NFC swelling on the rheological behaviour of high consistency furnishes

High consistency furnishes are flocculated suspensions of microfibrillar material (MFC and/or NFC), cellulose fibres and fillers, with a complex network matrix formed due to attractive interaction forces between its components. Their rheological behaviour is expected to depend on the solids concentration and the interaction of all the components. Data obtained from the amplitude sweep measurement on plate–plate rheometer presented in Fig. 2 show that MFC based furnishes have higher G' than the ones based on NFC, later having higher WRV (higher zeta potential), which has been observed before (Horvath and Lindström 2007). The test consisted of deformation sweep in order to determine linear viscoelastic regime. Furthermore, same figure shows that G' is higher for furnishes with cellulose fibres than those without cellulose fibers, increasing with consistency for all furnishes (Horvath and Lindström 2007). Figure 3 presents response of
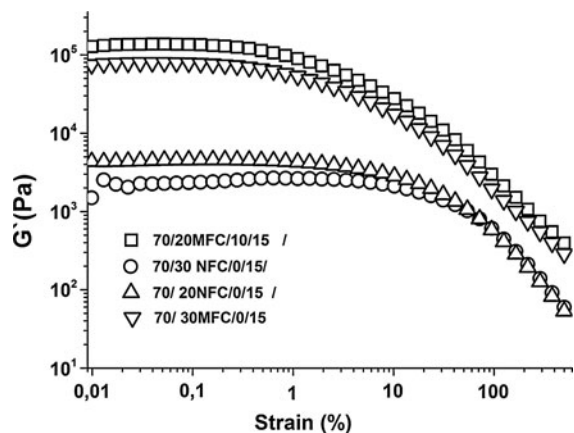
Fig. 2 G' in an amplitude sweep test for 15 % consistencies

dynamic moduli G' and G'' of 15 % consistencies furnishes as the functions of the frequency, for chosen representative result. As seen in the Fig. 3, consistent with results shown on previous figure, G' for NFC furnishes are generally lower than those of MFC furnishes, as more swollen NFC pronounce lower flocculation within furnish matrix(Horvath and Lindström 2007). The G' is nearly independent of the frequency, while the G'' is constant at low frequency and increases slightly at higher frequencies, tan δ being in between 0.2 and 0.3, in other word they behave as weak gels. Figure 4 depicts the average value of obtained from three frequency sweep measurements at 16 rad/s for all furnishes. This data further confirms the previous interpretation that the G' for MFC furnishes is higher compared to the NFC ones. Higher WRV of NFC implies that higher swelling and lower friction of
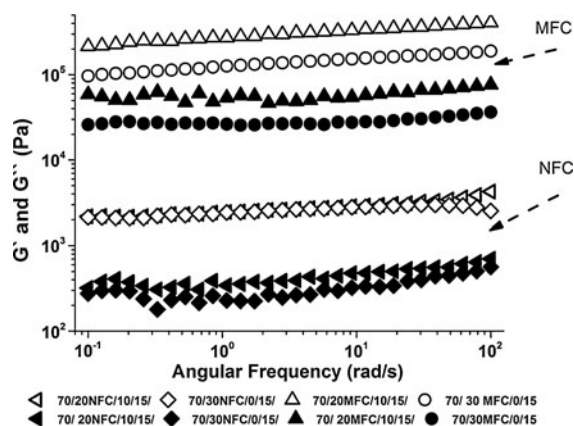
Fig. 3 G' and G'' in a frequency sweep test for 15 % consistencies furnishes, *open symbols* G', *closed symbols* G''
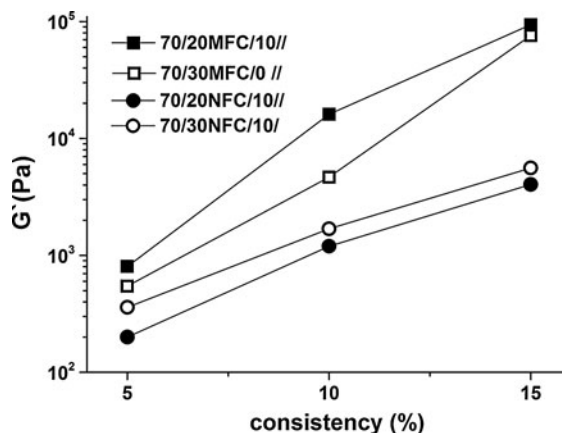
Fig. 4 G' at frequency 0.16 (s^{-1}) as functions of consistencies, for all furnishes

nanofibrillated cellulose within NFC furnish will result in weaker flocculation of the network matrix, which is seen as lower G' In general, the τ_c of flocculated suspension depends on the solids content, particle size distribution, and particle–particle interactions (Beghello and Eklund 1999; Karppinen et al. 2011; Richmond 2012, Richmond et al. 2012). The apparent τ_c for all furnishes is a function of consistency as plotted in Fig. 5. The apparent yield stress of all furnishes increases with consistency, which consistent with other research done on similar subject (Horvath and Lindström 2007); differences in τ_c between different furnish types are small at low solids content, but pronounced for highest solid content. When considering implementation of the shear in dewatering τ_c is an important parameter, as the structure of the sample evolves as the solid content increases. When the τ_c above the external stresses the flow stops (Gladman et al. 2005).

Shear thinning behaviour

Being viscoelastic, the structure of the flocculated network of MFC/NFC furnishes changes when it is sheared (Björkman 2005; Karppinen et al. 2011; Lasseuguette et al. 2008; Richmond 2012). The plot in Fig. 6 shows the steady state flow curves of MFC/NFC furnishes at shear rate 0.1–1,000 s^{-1}. All the furnishes are shear thinning, indicating the rupture of the flocculated network as the shear rate increases, typical for MFC/NFC suspensions. The flow curves show almost perfect power-law behaviour over three
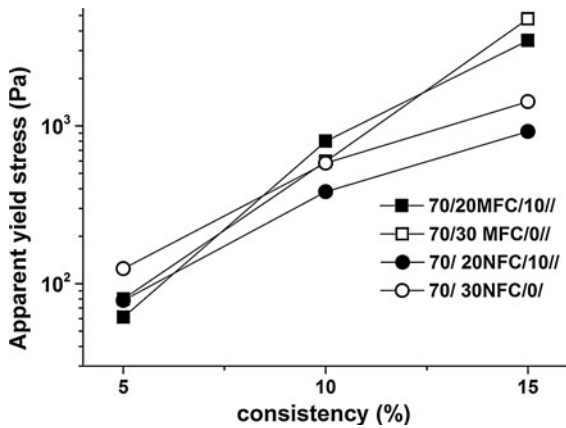
Fig. 5 Apparent τc from amplitude sweep test data. G' form linear viscoelastic region and Υ_c as a cross over point of tangents of two branches of G' *curves*

decades of shear rates between 1 and 1,000 s^{-1} and are, therefore, well described by the Ostwald Power Law (Eq. 2) (Lasseuguette et al. 2008; Richmond et al. 2012) .

$$\eta = K\dot{\gamma}^{-n} \qquad (2)$$

where η is the viscosity, Υ is the shear rate, and K and n are the flow index and the power-law exponent, respectively. Here $n = 0$ indicates a Newtonian fluid and $n < 0$ pseudo-plastic (shear thinning) behaviour.

All furnishes show shear thinning behaviour with $n \approx -1$, the actual fitted exponents vary between -1.02 and -0.94. The results show only weak dependence on the consistency in agreement to some earlier work (Lasseuguette et al. 2008; Puisto et al.
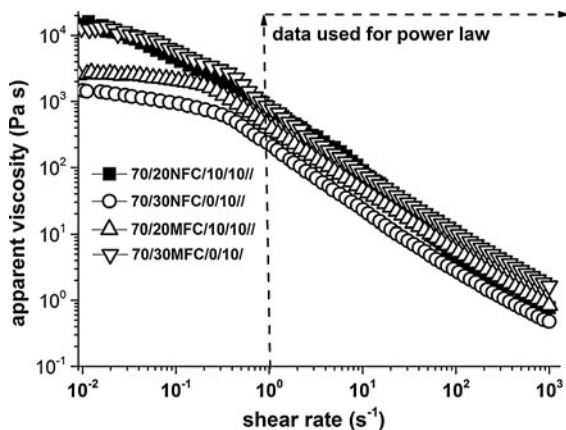
Fig. 6 Shear controlled test mode; all furnishes are presented in figure end their highly shear-thinning response to high shear
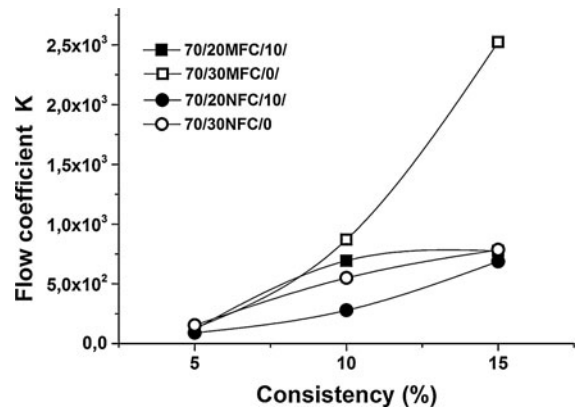
Fig. 7 K calculated with fitted $n = -1$

2012; Richmond et al. 2012). Therefore, we set $n = -1$ for all furnishes, and fit the data presented in Fig. 6 according to the power-law (Eq. 2) in order to obtain the K. The results are presented in Fig. 7 and Table 1. The relation between the K and consistency presented in Fig. 7, shows that the K increases with solids content, increase being more pronounced for furnishes containing no cellulose fibres.

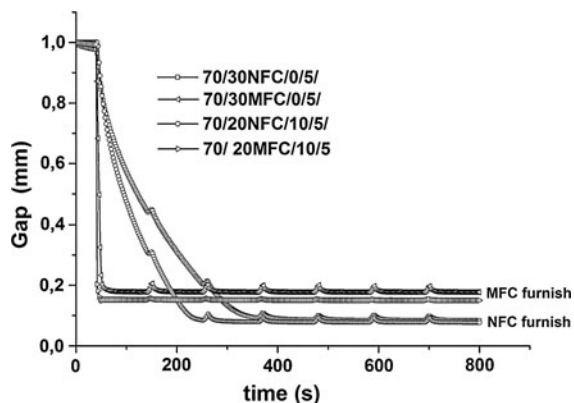Immobilization cell (IMC) dewatering

An IMC measurement can be defined (Willenbacher et al. 1999; Wollny 2001) as a process of measuring the increase of solid content by the increase of elastic moduli and viscosity during dewatering (Ayol et al. 2010; Jäder et al. 2003; Wollny 2001). Flow through the sample depends principally on the hydraulic pressure gradient, the porous microstructure of furnish, and the filter medium. We have extensively tested the effect of the filter medium to the experiment, and found that the particular filter we use is able to give the best reproducibility while still having a reasonably small flow resistance to allow measuring both nanocellulose types with good retention. In the MFC and NFC furnishes the dewatering of the sample may also stop at the point when the flow channels become sealed and the permeability effectively drops to zero. The curves plotted from IMC measurements are the average of 5 different measurements of the same furnish.

Data obtained from the DSO dewatering regime without rotation intervals shows the decrease of a gap after the onset of vacuum (after 40 s) during which the normal forces are expected to stabilize. The gap

Table 1 Calculated K for different furnishes at different consistencies for $n = -1$

Power law rheological model ($\eta = K\dot{\gamma}^{-n}$)		
Consistency (%)	Furnish name	Flow index K
5	70/20MFC/10/5	120
	70/30MFC/0/5	129
	70/20NFC/10/5	90
	70/30NFC/0/5	154
10	70/20MFC/10/10	693
	70/30MFC/0/10	870
	70/20NFC/10/10	279
	70/30NFC/0/10	549
15	70/20MFC/10/15	775
	70/30MFC/0/15	2,523
	70/20NFC/10/15	688
	70/30NFC/0/15	786

Fig. 8 Gap decrease for MFC and NFC furnishes at 5 % consistencies

decrease data plotted in Fig. 8 depicts that the gap decrease in initial stage (after application of vacuum), is steeper for furnishes containing cellulose fibres. This indicates that the pulp fibres influence positively on dewatering possibly by helping to create flow channels through the furnish cake. For the NFC based furnishes, the gap decrease in the initial stage of dewatering is slower than for the MFC furnishes. This is not surprising considering that the NFC is much more swollen and consists of finer elements than the MFC. The gap behaviour during dewatering plotted in Fig. 8 shows profound gap increase points, at the beginning of rotation, due to the response of highly viscoelastic structure to shear, i.e. the Weissenberg effect (Mezger 2006). The same tendency is observed for all furnishes, that the position at which the gap becomes constant is lower for the NFC furnishes than the MFC furnishes. Reasons for the difference in the final gap position, i.e. a lower final gap position for the NFC furnishes can be a higher solids content of the sample in the middle of the plate (Willenbacher et al. 1999), or different flocculation tendency upon shearing, both giving rise to viscoelastic response of dewatered sample. Therefore, the solids content of furnish cake, in case of our dewatering schemes cannot be calculated from the IMC measuring as a function of a gap decrease, i.e. dewatered volume (Jäder and Järnström 2003; Jäder et al. 2003; Pajari and Koskela 2010), as these results did not correlate with the dry

solids content measured gravimetrically using oven drying.

Our dewatering scheme utilises both testing approaches for IMC, the controlled shear rate (CSR), and the direct strain-controlled oscillatory (DSO) method. The CSR subjected furnish sample to rotation, while the vacuum dewatering was applied during the oscillation shearing in DSO. The DSO provides viscoelastic properties of the sample (G', G'' and complex viscosity (η^*)), while CSR provides only dynamic viscosity as the parameters of dewatering process. Therefore, for comparison purposes we chose to follow the increase in η^* (DSO) and change in η (CSR) to study dewatering kinetics. An increase of the solids content can be seen as an increase of η^*(DSO) (Jäder et al. 2003; Wollny 2001) and a decrease of η (CSR) (due to shear thinning), as presented in the rheogram at Fig. 9. Same figure depicts an increase in η^* during the DSO intervals and decrease of η during the CSR intervals, presented for 5 % consistencies NFC-furnishes containing no cellulose fibres, subjected under the shear rate of 200 s^{-1}. Both the η and η^* are dependent, and subjected to shear thinning, η^* to a smaller extent than η, as the sample is subjected to only mild oscillation during the DSO interval. Even though η^* increases throughout the measurement, however, its behaviour depends on many different viscoelastic factors, which also change with the solid content.
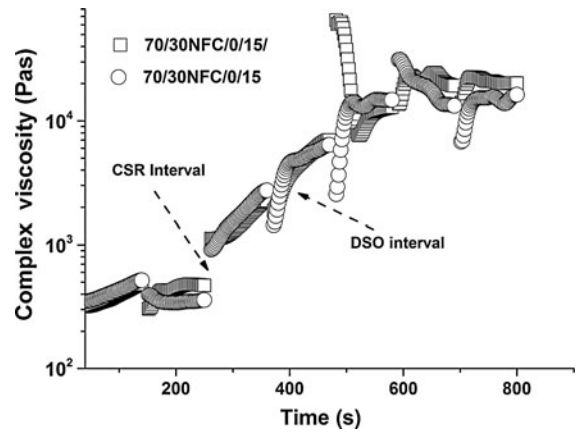
Figure 10 shows a η^* rheogram for 15 % NFC furnish, containing no cellulose fibers, for the shear rates (40 and 200 s^{-1}). Figure presents increase of the solids content through increase of the η^*(DSO), as
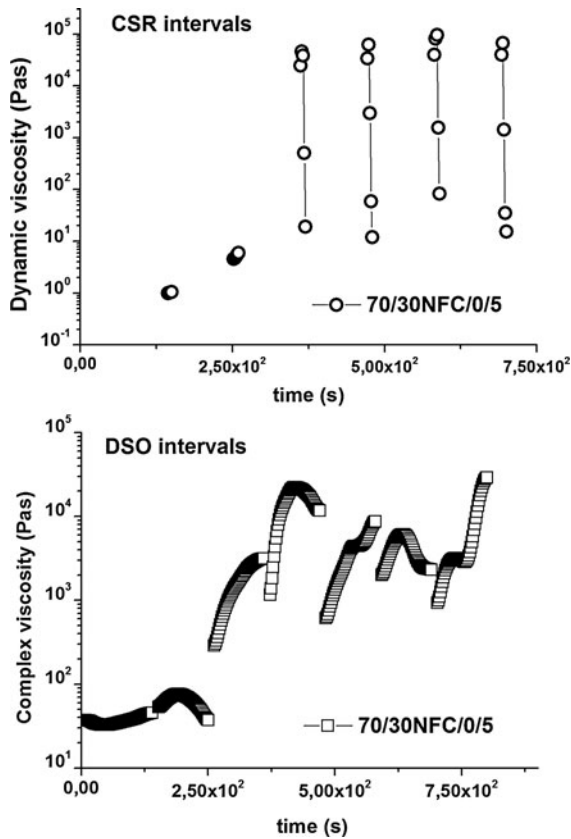
Fig. 9 Development of the η and $\eta*$ during the measurement of 5 % consistencies NFC-furnish without cellulose fibers, subjected to rotation rate of 200 s^{-1} during CSR cycle

Fig. 10 The $\eta*$ in DSO intervals for 15 % NFC furnish; data plotted are from DSO intervals while breaking points (empty places without data) are CRS intervals; circles shear rate 200 s^{-1} and squares shear rate 40 s^{-1}
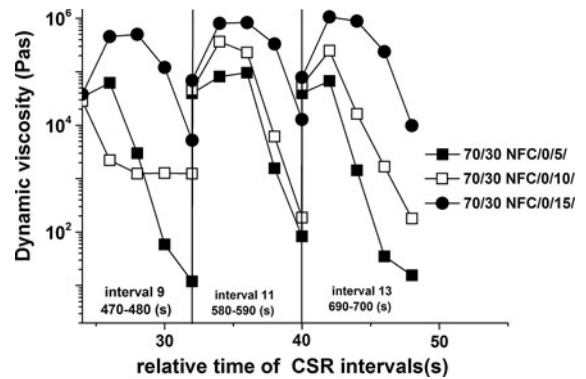

Fig. 11 η during last three CSR intervals for NFC furnishes with shear rate 200 s^{-1}; DSO interval are not plotted but marked with *vertical line*; time expressed as relative time of duration of the last intervals (9, 11, and 13) of measurement

studied earlier (Jäder et al. 2003; Wollny 2001). Apart from the first (pre-shearing) DSO interval, each following DSO interval is dependent on the visco-elastic response of furnish during the previous CSR intervals. During DSO interval $\eta*$ has a non-linear dependency on solids content of the furnish cake, shear thinning during the DSO interval, shearing history in previous CSR intervals, and the Weissenberg effect. In Fig. 11 are plotted the η data from the last three CSR intervals, from 470 to 800 s of the measurement, from the same NFC furnish at three different consistencies. An increase in the η at the beginning of rotation, due to Weissenberg effect, is followed by a profound shear thinning during all three intervals, for all imposed consistencies. Behaviour of η plotted in Fig. 11 shows that even that after many previous "initial dewatering" intervals (DSO),during which larger amount of water was removed, the shear thinning mechanism is very much present providing

further creation of dewatering channels. Both $\eta*$ and η (presented in Figs. 9, 10, 11) depend non-linearly on furnish consistencies, Weissenberg effect, shear thinning, and shear history. While the consistency changes only throughout the DSO interval (vaccum on), the viscoelastic effect is strongest during the beginning of CSR, while shear thinning and shear history change throughout the experiment (DSO and CSR intervals).

Data presented in Table 2 shows the increase of the solids content obtained by the different dewatering schemes. Data shows that increase in the solids content when rotation intervals are applied is two times higher than in cease were dewatering was performed without rotation. We believe that the reason for this is that the

Table 2 The final solids contents of furnish cake after 800 s

Furnish name		No rotation, vaccum on/off (DSO) Final solid content (%)	CSR 40 s^{-1} Final solid content (%)	CSR 200 s^{-1} Final solid content (%)
5	70/20MFC/10/5	19.2	26.3	28.7
	70/30MFC/0/5	17.5	22.5	32.1
	70/20NFC/10/5	16.3	22.3	26.3
	70/30NFC/0/5	14	21.6	26.1
10	70/20MFC/10/10	19.4	26.4	29.4
	70/30MFC/0/10	17.2	24.6	28.6
	70/20NFC/10/10	16.4	25.4	29.4
	70/30NFC/0/10	14	24.5	29.1
15	70/20MFC/10/15	23.5	28.3	34.4
	70/30MFC/0/15	22.3	27.9	33..4
	70/20NFC/10/15	21.4	27.9	33.2
	70/30NFC/0/15	20	27.5	32.1

Fig. 12 Solid content increase $\Delta\varphi$, for different dewatering schemes versus shear rates in CSR intervals 0, 40 and 200 s^{-1}, and the K for all furnishes
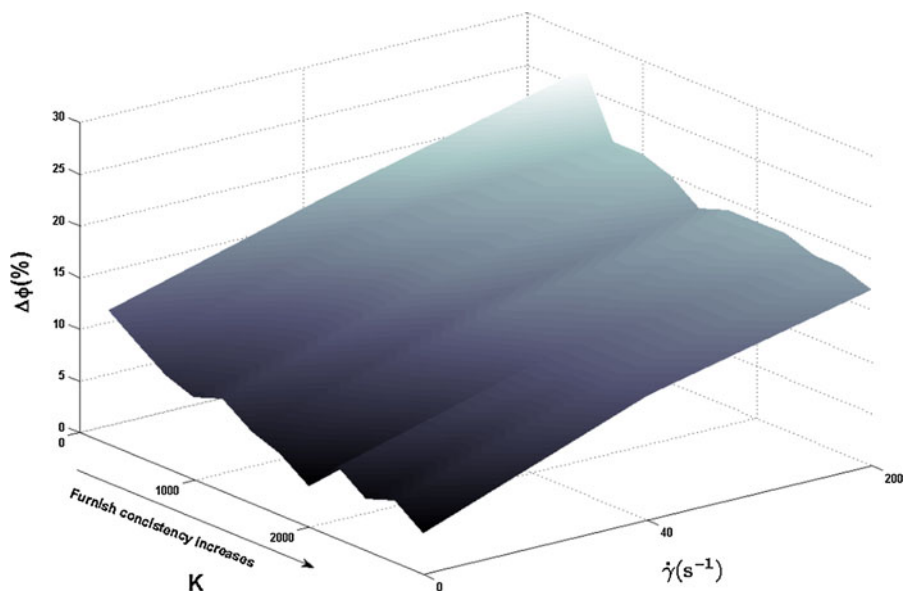
function of shear in the CRS interval is to brake the flocculated matrix of the dewatering furnish cake, enabling phase separation between water and other components. The amount of shear imposed on the furnish cake sample affects the shear thinning behaviour, as a response to the shear being different between furnishes, seen as a K, as in Fig. 3b.

Figure 12 shows the final solids content increase of the dewatered samples as a function of shear rate (dewatering scheme) and the K. As this figure depicts, applying a higher shear rate results in a solids content

increase regardless of the MFC/NFC type and whether cellulose fibres are present or not. Increase in solids content is always highest for lowest furnish consistencies (5 %), and decreases with increase in furnish consistencies, for all three shear rates.

Conclusions

This study introduces a new rheological method to evaluate the dewatering and rheological behaviour of

high consistency MFC/NFC furnishes simultaneously. Using this method, the rheological behaviour of furnishes was found to be influenced by the type of nanocellulose. Flow curves of both the MFC and NFC suspensions and furnishes showed gel-like structure, shear thinning behaviour and had a high τ_c.

The IMC enables the application of vacuum dewatering under shear. This is a significant advantage when trying to understand the application of shear as a means to improve the dewatering of the MFC/NFC furnishes. The implementation of rotation cycles in between the oscillation vacuum cycles was found to increase the final solids content of the samples. Minute difference in the final solids content was obtained with respect to the MFC/NFC type and the presence of cellulose fibres. The very high elasticity of the MFC/NFC furnishes results in the Weissenberg effect during shearing, thus making it difficult to follow the solids content increase directly from the gap size.

During the dewatering measurement, the solids content of the sample increases, and so does its yield stress. The shear thinning behaviour of furnish has an important relationship to dewatering. When the microstructure of the suspension is broken by the shear field, the process is able to propagate out flow channels in the pad. Thus, the repeated shear cycles aid in the dewatering. It was found that the dewatering becomes more efficient at shear rates. This is due to the fact that the shear thinning is almost without exception related to the breakage of the suspension internal structure, freeing parts of the internally jammed water. Free water can then be easily removed from the fluid by a simple vacuum suction. However, there are limitations related to this method. First, the Weissenberg effect, which tends to distribute the solids on the rheometer plate unevenly, increases with the shear rate. Second, as the structure of the solid phase is broken into small parts, there is a risk that these penetrate the cake and the filter, therefore reducing the solids retention. Taking these limitations into account, the presented method of implementation of shear in between vacuum cycles can be applied where efficient dewatering of high consistency furnishes is needed.

References

Agoda-Tandjawa G, Durand S, Gaillard C, Garnier C, Doublier J- (2012) Rheological behaviour and microstructure of microfibrillated cellulose suspensions/low-methoxyl pectin mixed systems. Effect of calcium ions. Carbohydr Polym 87:1045–1057

Ayol A, Dentel SK, Filibeli A (2010) Rheological characterization of sludges during belt filtration dewatering using an immobilization cell. J Environ Eng 136:992–999

Barnes HA (2007) The 'yield stress myth?' paper—21 years on. Appl Rheol 17:43110-1-43100-5

Barnes H, Carnali J (1990) The vane-in-cup as a novel rheometer geometry for shear thinning and thixotropic materials. J Rheol 34:841

Beghello L, Eklund D (1999) Influence of the chemical environment on fibre flocculation. J Pulp Paper Sci 25:246–250

Björkman U (2005) Floc dynamics in flowing fibre suspensions. Nord Pulp Pap Res J 20:247–252

Blanco A, Negro C, Fuente E, Tijero J (2007) Rotor selection for a Searle-type device to study the rheology of paper pulp suspensions. Chem Eng Process 46:37–44

Chinga-Carrasco G, Kuznetsova N, Garaeva M, Leirset I, Galiullina G, Kostochko A, Syverud K (2012) Bleached and unbleached MFC nanobarriers: properties and hydrophobisation with hexamethyldisilazane. J Nanopart Res 14:1280

Dolz M, González F, Herráez M, Díez-Sales O (1994) The influence of starch on the rheological behaviour of microcrystalline cellulose hydrogels. J Dispersion Sci Technol 15:189–205

Dursun D, Dentel SK (2008) New rheological method to evaluate the dewaterability of biosolids. Proceedings of the water environment federation 2008:24–36

Gladman B, De Kretser R, Rudman M, Scales P (2005) Effect of shear on particulate suspension dewatering. Chem Eng Res Design 83:933–936

González I, Boufi S, Pèlach MA, Alcalà M, Vilaseca F, Mutjé P (2012) Nanofibrillated cellulose as paper additive in eucalyptus pulps. BioResources 7:5167–5180

Henriksson M, Henriksson G, Berglund L, Lindström T (2007) An environmentally friendly method for enzyme-assisted preparation of microfibrillated cellulose (MFC) nanofibers. Eur Polymer J 43:3434–3441

Horvath AE, Lindström T (2007) The influence of colloidal interactions on fiber network strength. J Colloid Interface Sci 309:511–517

Hubbe MA, Heitmann JA (2007) Review of factors affecting the release of water from cellulosic fibers during paper manufacture. BioResources 2:500–533

Hubbe MA, Panczyk M (2007) Dewatering of refined, bleached hardwood kraftpulp by gravity, vacuum, and centrifugation with applied pressure part 2. Effects of wet-end additives. O Papel (Brazil) 68:88–100

Iotti M, Gregersen ØW, Moe S, Lenes M (2011) Rheological studies of microfibrillar cellulose water dispersions. J Polym Environ 19:137–145

Jäder J, Järnström L (2003) The influence of thickener addition on filter cake formation during dewatering of mineral suspensions. Appl Rheol 13:125–131

Jäder J, Järnström L, Engström G (2003) The immobilization cell revisited: prediction of dewatering kinetics and immobilised layer properties for coating colours. Nordic Pulp Paper Res J 18:382–387

Karppinen A, Vesterinen AH, Saarinen T, Pietikäinen P, Seppälä J (2011) Effect of cationic polymethacrylates on the

rheology and flocculation of microfibrillated cellulose. Cellulose 18:1381–1390

Lasseuguette E, Roux D, Nishiyama Y (2008) Rheological properties of microfibrillar suspension of TEMPO-oxidized pulp. Cellulose 15:425–433

Lindström T, Carlsson G (1982) The effect of chemical environment on fiber swelling. Svensk Papperstindning-Nordisk Cellulosa 85:14–20

Mezger TG (2006) The rheology handbook: for users of rotational and oscillatory rheometers. Vincentz Network GmbH & Co KG, Hannover

Nakagaito AN, Fujimura A, Sakai T, Hama Y, Yano H (2009) Production of microfibrillated cellulose (MFC)-reinforced polylactic acid (PLA) nanocomposites from sheets obtained by a papermaking-like process. Compos Sci Technol 69:1293–1297

Ovarlez G, Rodts S, Chateau X, Coussot P (2009) Phenomenology and physical origin of shear localization and shear banding in complex fluids. Rheol Acta 48:831–844

Pajari H, Koskela H (2010) 9.2—Consolidation of coating colors—Experimental studies. 11th advanced coating fundamentals symposium proceedings: the latest advances in coating research and development: 347–359

Paradis MA, Genco JM, Bousfield DW, Hassler JC, Wildfong V (2002) Determination of drainage resistance coefficients under known shear rate. Tappi J 1:12–18

Puisto A, Illa X, Mohtaschemi M, Alava M (2012) Modeling the viscosity and aggregation of suspensions of highly anisotropic nanoparticles. Eur Phys J E 35:1–7

Pujara J, Siddiqui M, Liu Z, Bjegovic P, Takagaki S, Li P, Ramaswamy S (2008) Method to characterize the air flow and water removal characteristics during vacuum dewatering. Part II—analysis and characterization. Drying Technol 26:341–348

Raisanen KO, Paulapuro H, Karrila SJ (1995) The effects of retention aids, drainage conditions, and pretreatment of slurry on high-vacuum dewatering: a laboratory study. Tappi J 78:140–147

Ramaswamy S (2003) Vacuum dewatering during paper manufacturing. Drying Technol 21:685–717

Renardy M (2010) The mathematics of myth: yield stress behavior as a limit of non-monotone constitutive theories. J Non Newtonian Fluid Mech 165:519–526

Richmond F (2012) The coating of nanofibrillated cellulose onto paper using flooded and metered size press methods. 12PaperCon/Papers/12PAP18 aspx

Richmond, Finley-Co, Abert-Bousfield Douglas (2012) The coating of nanofibrillated cellulose onto paper using flooded and metered size press methods. 12 paperCon/Papcrs/12 PAP18 aspx

Saito T, Isogai A (2005) TEMPO-mediated oxidation of native cellulose. Appita Annual Conference 3:337–340

Siró I, Plackett D (2010) Microfibrillated cellulose and new nanocomposite materials: a review. Cellulose 17:459–494

Spence KL, Venditti RA, Rojas OJ, Habibi Y, Pawlak JJ (2010) The effect of chemical composition on microfibrillar cellulose films from wood pulps: water interactions and physical properties for packaging applications. Cellulose 17:835–848

Subramanian R, Hiltunen E, Gane PAC (2011) Potential use of micro- and nano-fibrillated cellulose composites exemplified by paper. Cellulose fibers: bio-and nano-polymer composites. Green Chem Technol 121

Turbak AF, Snyder FW, Sandberg KR (1984) Microfibrillated cellulose—A new composition of commercial significance: TAPPI 1984, Conference Proceedings, Nonwovwns Symposium Notes, pp 115–123

Walls HJ, Caines SB, Sanchez AM, Khan SA (2003) Yield stress and wall slip phenomena in colloidal silica gels. J Rheol 47:847–868

Willenbacher N (2011) Novel approaches to explain the rheological properties of colloidal structures. Curr Opin Colloid Interface Sci 16:1–2

Willenbacher N, Hanciogullari H, Radle M (1999) New laboratory test to characterize immobilization and dewatering of paper coating colors. Tappi J 82:167–174

Wollny K (2001) New rheological test method to determine the dewatering kinetics of suspensions. Appl Rheol 11:197–202